Antibody-Targeted Nanovectors for the Treatment of Brain Cancers

Martyn A. Sharpe,[†,*] Daniela C. Marcano,[‡] Jacob M. Berlin,[‡] Marsha A. Widmayer,[†] David S. Baskin,[†] and James M. Tour[‡,§,*]

[†]Department of Neurosurgery, Methodist Hospital, 6560 Fannin Street, Houston, Texas 77030, United States, and [‡]Department of Chemistry and the [§]Smalley Institute for Nanoscale Science and Technology, Rice University, MS-222, 6100 Main Street, Houston, Texas 77005, United States

ABSTRACT

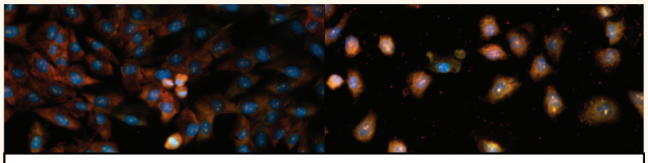

GBM cells treated with 0.5 μM Vinblastine/PEG-HCCs, in the absence (left) and presence (right) of anti-EGFR IgG. Dead and dying GBM cells are RBG labeled with *dd*TUNEL (red) and viability dyes Dead Green and Hoechst (blue).

Introduced here is the hydrophilic carbon clusters (HCCs) antibody drug enhancement system (HADES), a methodology for cell-specific drug delivery. Antigen-targeted, drug-delivering nanovectors are manufactured by combining specific antibodies with drug-loaded poly(ethylene glycol)—HCCs (PEG—HCCs). We show that HADES is highly modular, as both the drug and antibody component can be varied for selective killing of a range of cultured human primary glioblastoma multiforme. Using three different chemotherapeutics and three different antibodies, without the need for covalent bonding to the nanovector, we demonstrate extreme lethality toward glioma, but minimal toxicity toward human astrocytes and neurons.

KEYWORDS: glioblastoma multiforme · nanovectors · hydrophilic carbon clusters · drug delivery

Glioblastoma multiforme (GBM) is the most common and aggressive malignant primary brain tumor in humans. GBM prognosis is poor, with a 14-month median survival time despite interventions.[1] Nanovectors, nanoparticles capable of transporting and delivering drugs and bioactive molecules, are an emerging class of drug-delivery platforms.[2] Some nanovectors, such as hydrophilic carbon clusters (HCCs)[3−5] and single-walled carbon nanotubes,[6] can be engineered to possess both hydrophobic and hydrophilic domains, combining high aqueous solubility with the ability to adsorb hydrophobic compounds. Therefore nanovectors are an exciting avenue for drug delivery of such compounds without the need for covalent drug or covalent antibody attachment[6,7] and could be used to target glioma.[7−11]

HCCs are heavily oxidized carbon nanoparticles that are 30 to 40 nm long and approximately 1 nm wide, and although water-soluble, they must be further functionalized with poly(ethylene glycol) (PEG-5000) to maintain their solubility in phosphate-buffered saline (PBS), thereby rendering the PEG-HCCs nanovector system. Their synthesis and characterization have been described previously.[3,4] PEG—HCCs have three properties that allow them to be used as nanovectors: extremely low biological toxicity with clearance mainly through the kidneys,[3] hydrophobic domains of the PEG—HCCs that can be noncovalently loaded with drugs,[3,5] and an ability to strongly bind to IgG-type antibodies while the antibodies maintain the majority of their activity.[4,5] Thus, drug-loaded PEG—HCCs combined with an IgG will bind to a chosen cell surface antigen and deliver a hydrophobic, lipophilic drug into cells that express the selected epitope. We use the nomenclature $Epitope_{AB}$/Drug/PEG—HCCs to describe a particular hydrophilic carbon cluster antibody enhancement system (HADES) composed of an antibody, a drug, and the PEG—HCCs delivery platform. In this nomenclature, noncovalent sequestration is indicated with a slash, "/", and covalent bonding with a dash, "—". In each case, the drug and the antibody are added, sequentially, to the PEG—HCCs by simple mixing; hence a facile "mix-and-treat" toolbox is afforded.[4]

We have sequestered three potent hydrophobic chemotherapeutic agents onto the PEG—HCCs, chosen on the basis of theoretical synergistic effect. These include (a) SN-38, a topoisomerase I inhibitor, which arrests the cell cycle in the S and G2 phases,[12] (b) vinblastine (Vin), which causes microtubule detachment from spindle poles, arresting the cell cycle in the M phase at the mitotic

* Address correspondence to msharpe@tmhs.org, tour@rice.edu.

Received for review December 12, 2011 and accepted March 5, 2012.

Published online March 05, 2012
10.1021/nn2048679

© 2012 American Chemical Society

spindle checkpoint,[13] and (c) docetaxel (Doc), which binds tubulin, preventing microtubule depolymerization and arresting the cell cycle in both the G2 and M phases, resulting in mitotic catastrophe.[14] Of note, SN-38 is dramatically more potent than the pro-drug form, Irinotecan, but SN-38 cannot be directly administered to patients due to its extremely low aqueous solubility.[15] The use of the HADES system allows for the direct delivery of this active drug, and perhaps other pharmaceutics, whose solubility requires the use of moieties that increase solubility but limits drug efficacy.

To treat GBM, we selected immunoglobulin G antibodies (IgGs) to cell surface epitopes that are overexpressed in glioma cells relative to other cell types. $GFAP_{AB}$ is an IgG-type antibody to the glial fibrillary acidic protein (GFAP), a protein present in reactive astrocytes and also highly expressed in the majority of GBM cells.[16] The interleukin-13 receptor (Il-13R) is a cytokine receptor, binding interleukin-13, and has been found to be upregulated in a large range of cancers, including GBM.[17] Normal, unreactive, astrocytes express low levels of GFAP[18,19] and even lower levels of IL-13R.[20] The epidermal growth factor receptor (EGFR) is the cell-surface receptor for members of the EGF family of extracellular proteins. This receptor is overexpressed, in either full length or truncated form, in many cancers including GBMs.[21] Surface epitope mapping was performed on primary glioma cell cultures, and the binding of specific IgGs to GFAP: IL-13R:EGFR had ratios of 1.0:1.3:1.6, respectively (Figure S1a–c).

We examined the effectiveness of the antibody-targeted, IgG/drug/PEG–HCCs in primary human glioma cultures and control cultures of normal human astrocytes (NHA) and human cortical neurons (HCN). As GBM generates blood–brain barrier defects, this antibody-guided drug-delivery system might ultimately be used intravenously to actively target glioma cells.[22]

In Figure 1a we demonstrate the ability of the HADES formulation $GFAP_{AB}$/SN-38/PEG–HCCs, with each component concentration at 3.9 nM, 2 μM, and 2.6 nM, respectively, to induce cell death in primary GBM cell cultures. Due to the fact that nanomaterials can often interfere with biological assays,[23] three different methodologies were used to measure cell viability. Total, viable, and dead gliomal cell numbers in confluent primary GBM cell cultures were measured using *dd*TUNEL (a quantitative assay for 3′OH DNA ends),[24] Dead Green,[25] and Hoechst stains.[24] Cells were treated with $GFAP_{AB}$/SN-38/PEG–HCCs or saline for 24 h. SN-38-induced cell death could be monitored by all three viability methodologies, but there was slight under-reporting of total cell numbers using both *dd*TUNEL and Dead Green, with respect to Hoechst, due to the presence of overlapping cells.[26] It is clear

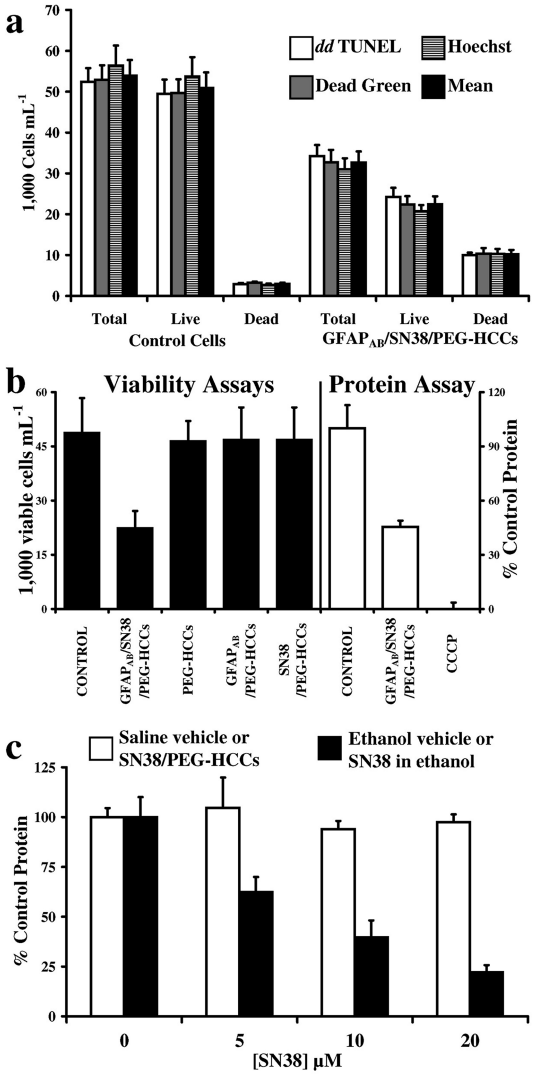

Figure 1. Four measures of viability all show that HADES therapy kills GBM primary cultures. (a) The three cell viability measures, *dd*TUNEL (white bars), Dead Green (gray bars), and Hoechst staining (striped bars), all give similar live/dead numbers (averages are the black bars) in GBM cultures in the absence (controls, left) and presence (HADES, right) of $GFAP_{AB}$/SN-38/PEG–HCCs with each component at the following concentrations: 3.9 nM, 2.6 nM, and 2 μM, respectively. Viable cell numbers fall to only 44% of the control in HADES-treated cells, and the dead cell fraction rises from 5.5% to 31%. (b) Average levels of living GBM cells (left), from *dd*TUNEL, Dead Green, and Hoechst staining, show that the individual HADES components, PEG–HCCs, $GFAP_{AB}$/PEG–HCCs, and SN-38/PEG–HCCs are nontoxic, whereas HADES treatment, in the form of $GFAP_{AB}$/SN-38/PEG–HCCs, causes significant cell death. Additionally, changes in cell protein mass, using the BCA method (right panel), correlate with viable cell numbers determined using viability stains in fixed cells, using the lethal uncoupling agent CCCP to establish the minimum cellular protein levels. (c) Comparison of SN-38 toxicity when presented to GBM in solution or as HADES. SN-38 is insoluble in water, so it had to be delivered in ethanol and was compared to an ethanol control. Thus, changes in protein mass after 24 h treatment with SN-38/PEG–HCCs (white bars) and SN-38 (black bars) were compared to saline or ethanol only controls, respectively. SN-38/PEG–HCCs are not toxic up to 20 μM SN-38, whereas aqueous SN-38 has an LD_{50} of ~8 μM. In all figures $n = 8$ wells and the error bars are equal to the SD.

that the three methodologies are robust even in the presence of nanomolar concentrations of PEG–HCCs. Figure 1a further shows that in the saline control viable cell numbers increased from the ~30 000 inoculum to 52 000 cells mL^{-1} in 24 h, whereas incubation with $GFAP_{AB}$/SN-38/PEG–HCCs showed a decrease in cell numbers to only 22 000 cells mL^{-1}. Moreover, there was a 3-fold increase in the number of dead cells following treatment with HADES.

Figure 1b (left panel) shows that the individual components of HADES treatment, PEG–HCCs (2.6 nM), $GFAP_{AB}$ (3.9 nM), and SN-38 (2 μM), are not toxic toward cells when added individually. Only when the three components, targeting antibody, chemotherapeutic, and nanovector, are all combined is there an increase in cell death. Addition of the three individual HADES components to glioblastoma cells results in no statistically significant difference in cell viability. Remarkably, we find that PEG–HCCs alone are not toxic toward glioma, astrocytes, or neurons at concentrations more than 3 orders of magnitude greater than those used in all the experiments related to Figure 1 (Figure S2). This corresponds with previous reports showing that PEG–HCCs are not toxic to mammalian cell cultures or in mice.[3−5]

Cell counting assays are time-consuming; in order to validate a high data throughput assay, we compared the changes in cell numbers obtained from viability studies with the use of the bicinchoninic acid (BCA) assay of protein levels (Figure 1b). The maximum and minimum cellular protein levels were established using a saline negative control (100%) and carbonyl cyanide chlorophenyl hydrazone (CCCP) positive control (0%). Incubation of GBM for 24 h with CCCP (100 μM) induces cell death by mitochondrial uncoupling and allows the background matrix protein levels to be determined. Cellular protein levels following HADES treatment fell to 46% of the saline control level, mirroring the 44% levels of living cells determined using viability methodologies.

The impact of sequestering SN-38 on the hydrophobic core of the PEG–HCCs was evaluated by comparing the changes in cellular protein of GBM following 24 h incubation with SN-38/PEG–HCCs or SN-38 alone (Figure 1c). As mentioned previously, SN-38 is extremely insoluble in water;[15] for this reason, in experiments using bulk phase drug we added either 5 μL of ethanol or ethanol containing SN-38 to each 250 μL well volume. The two controls, ethanol and saline, had no significant change in cellular protein relative to one another. We found that aqueous SN-38 has an LD_{50} of approximately 8 μM toward primary GBM, within the 5–10 μM range reported by others using immortalized human glioblastoma cell cultures.[27] Interestingly, no toxicity is observed when SN-38 is presented to the cells in the form of SN-38/PEG–HCCs, even at concentrations as high as 20 μM. This indicates

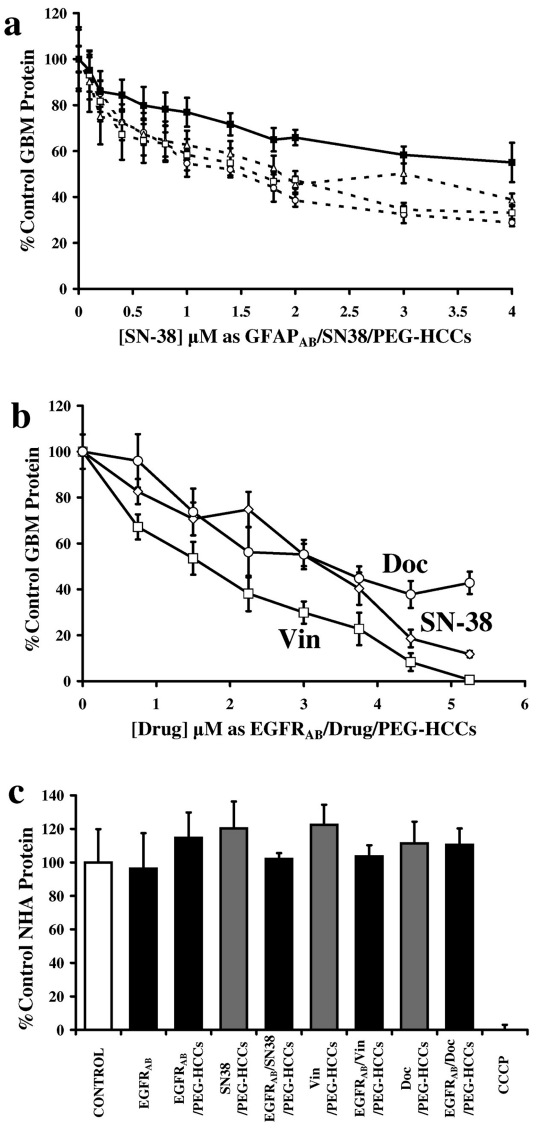

Figure 2. HADES therapy is highly versatile, having broad antibody/drug specificity, and it is lethal toward a range of GBM. (a) The dose–response curve of three different GBMs (dashed lines) and one anaplastic astrocytoma (solid line) toward anti-$GFAP_{AB}$/SN-38/PEG–HCCs, measured at 24 h. (b) HADES treatment using three hydrophobic drugs: Vin (□), Doc (○), and SN-38 (◊) were presented to GBM for 24 h within PEG–HCCs, targeted to the tumor antigen, EGFR, by an IgG. (c) Astrocytes are insensitive to HADES and the individual HADES components, as shown by protein measurement following 24 h incubation. Control (white bar on left), incubation of NHA with $EGFR_{AB}$ and $EGFR_{AB}$/PEG–HCCs (next two black bars) and then with $EGFR_{AB}$ in the absence (gray bars) and presence (black bars) of PEG–HCCs ± drug (5 μM) causes no change in protein mass.

that the SN-38/PEG–HCCs, without antibody targeting, cannot deliver the drug to the GBM cells at any significant rate.

In Figure 2 we show that HADES treatment is toxic toward a variety of human glial cell carcinomas and that the system is flexible with respect to the loaded chemotherapeutic. In Figure 2a we show the titration of three different primary GBM cultures, and one primary

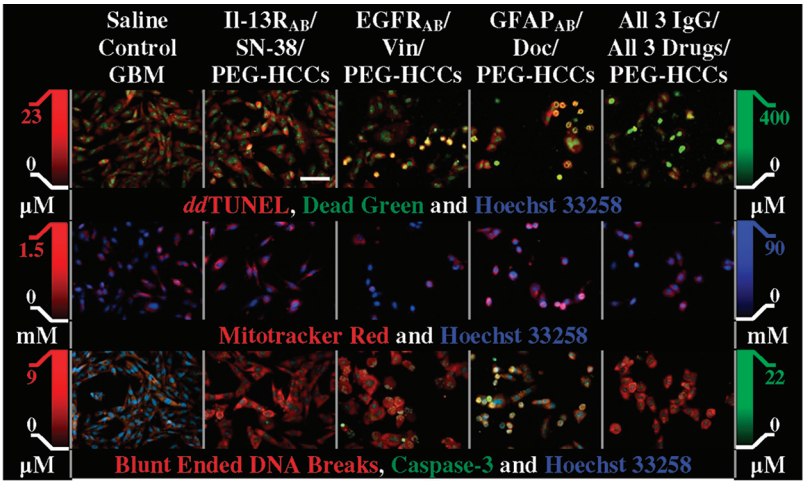

Figure 3. Effects of Vin, Doc, and SN-38 HADES individual or triple therapy on GBM measured using six different death markers; all drugs at a final concentration of 0.5 μM. The upper row shows 3′OH DNA ends, Dead Green, and Hoechst DNA staining, the middle row shows mitochondrial membrane potential, and the bottom row shows blunt-ended, lethal, DNA breaks[24,28] and caspase-3 activity. All of the figures are at 20× magnification, and the side bars show the calibration scale for each fluorophore.[24,28]

anaplastic astrocytoma (solid line), with GFAP$_{AB}$/SN-38/PEG−HCCs. The three GBM cultures, which have a doubling time of 28 to 34 h, have a common dose response with a LD$_{50}$ of 1.5 to 2 μM SN-38, delivered in the form of HADES. In the slower growing anaplastic astrocytoma, which has a doubling time of 48 to 52 h, the LD$_{50}$ is elevated to ~3.75 μM SN-38. In Figure 2b we show the dose response of GBM toward three different chemotherapeutics, SN-38, Vin, and Doc, which were loaded into PEG−HCCs and guided to the cell membrane using EGFR$_{AB}$. The highest concentration of GFAP$_{AB}$ used on the confluent cells was 10 nM. In control experiments, the incubation was 1 h with GFAP$_{AB}$/SN-38/PEG−HCCs, with each component concentration at 10 nM, 5 μM, and 6.5 nM, respectively. Then, fixed cells were stained using a labeled goat anti-mouse secondary antibody. Results indicated 86% saturation of the total surface GFAP epitopes, indicating that only 14% of the surface epitope is not bound to GFAP$_{AB}$/SN-38/PEG−HCCs (Figure S1d). Using this nanovector delivery system, the LD$_{50}$ for both SN-38 and Vin is ~1.5 μM, while for Doc it is ~3 μM.

In Figure 2c we show the effects of 5 μM drug/PEG−HCCs ± EGFR$_{AB}$ treatment on normal human astrocyte total protein levels, a treatment that caused >85% cell death in glioma. Neither PEG−HCCs nor EGFR$_{AB}$/PEG−HCCs cause cell death. Extraordinarily, astrocytic mass was unaffected by the three EGFR$_{AB}$/drug/PEG−HCCs combinations, each of which was overwhelmingly lethal to GBMs.

Clinically, the use of combined therapy in cancer treatment is an attempt to evade the heterogeneous response that a cancer cell population has toward different chemotherapeutics and the ability of cancer cells to rapidly acquire drug resistance. As SN-38, Vin, and Doc all have different pharmacologic targets, we postulated that the three drugs might be able to potentiate each other's anticancer properties. We incubated GBM, and also control NHA and HCN, with low levels of the three drugs in HADES form, consisting of three individual HADES formulations and an additional triple combination therapy where the three HADES individuals were combined (Figure 3). The low drug levels chosen, 0.5 μM, allowed enough damaged and dying cells to remain at the end of a 24 h incubation to be characterized using specific probes of DNA damage, mitochondria dysfunction, loss of plasma membrane potential, and the initiation of apoptotic, proteolytic, cascades.

The upper panel of Figure 3 shows the effects of the individual drugs and triple therapy on the viability of glioma primary cultured GBM cells, demonstrated by *dd*TUNEL (red)[24] and Dead Green and Hoechst (blue). It is evident that both Vin and Doc have devastating impacts on GBM. Microscopic examination shows evidence of mitotic catastrophe and of the presence of gear-wheel-shaped nuclei, typical of the microtubule-disrupting actions of Vin[29] and Doc.[14,30] The center panel of Figure 3 shows the loss of mitochondrial membrane potential with all four HADES regimes. Vin has been shown to alter the distribution of mitochondria throughout cells and to cause mitochondrial "clumping",[31] and this type of mitochondrial flocculation is clearly evident in GBM. We also observe changes in mitochondrial morphology and cytosolic distribution in GBM treated with EGFR$_{AB}$/Doc/PEG−HCCs that are very similar to those observed in prostate cancer cells treated with taxels.[30]

The lowest panels of Figure 3 show the levels of blunt-ended DNA breaks[24,28] and caspase-3 activity. All three individual HADES therapies cause increases in these lethal DNA breaks and in apoptotic, caspase-3 activity.[32] EGFR$_{AB}$/Doc/PEG−HCCs in particular increases caspase-3 activation, especially in the condensed cells, in which gear-wheel-shaped nuclei predominate. In Figure S3a−c, we show the death labeling of two more primary GBMs and that of an anaplastic astrocytomoa,

under conditions identical to that of Figure 3. In addition in Figure S3d–e, we show the effects of the same therapies on cultures of NHA and HCN. In stark contrast to the effects of HADES on GBM, the effects on astrocytes and neurons are far more modest. Compared to control, for the four treatment groups, there is a doubling in the levels of *dd*TUNEL-positive DNA 3′OH ends in NHA but no great increase in cell death. In Figure S3e, it is noteworthy that we observe no changes in nuclear structure of the treated neurons, even though neurons are very vulnerable toward microtubule disruption drugs such as Doc[30] and Vin (Figure S3f).[33]

Figure 4 shows the extent of cell viability and death, for GBM, NHA, and HCN, using Hoechst staining. Figure 4a shows the levels of live and dead GBM cells following individual HADES treatments and the triple therapy. The two microtubule-targeting chemotherapeutics are much more effective than the topoisomerase-I inhibitor, SN-38. Treatment with Il-13R_{AB}/SN-38/PEG–HCCs, $GFAP_{AB}$/Vin/PEG–HCCs, or $EGFR_{AB}$/Doc/PEG–HCCs all produced a statistically significant, $p < 0.01$, drop in living cell numbers and an increase in dead cell percentages. There is a statistically significant, $p < 0.01$, synergistic effect caused by triple therapy, with respect to the individuals, on the level of cell death.

With respect to NHA and HCN, HADES treatment did not result in statistically significant changes in cell viability. However, in the case of HCN, only four wells were used for each treatment. Therefore, the number is too low to make accurate statistical assertions. We therefore measured the changes in HCN protein levels in controls and following HADES treatment [as we had done with NHA (Figure 2c)], and we present these data in Figure S4. The BCA assay shows that individual HADES therapies do not kill neurons, to any statistically significant degree, when using protein as a measure of cellular mass. However, combining the three drug-loaded PEG–HCCs, in the absence or presence of antibodies, does cause a statistically significant, $p < 0.05$, drop in cell protein levels. In spite of this increase in the killing of neurons, use of a multipronged therapy often has utility in treatment due to its potential ability to avoid the development of drug resistance.

In summary, we are able to target drug-loaded PEG–HCCs to the surface epitopes of cells, using specific antibodies. EGFR,[34] IL-13R,[35] and GFAP[36] are not present in human cortical neurons, but are found in high levels in GBM.[34–36] Single or triple therapy is capable of killing gliomas with extreme lethality, while at the same time causing little or no ill-effects toward either astrocytes or neurons. The simplicity of the preparation where the PEG–HCCs, drug, and antibody are simply mixed together, coupled with the lethality of these combinations toward extremely aggressive cancers, provides encouragement for the continued testing of HADES.

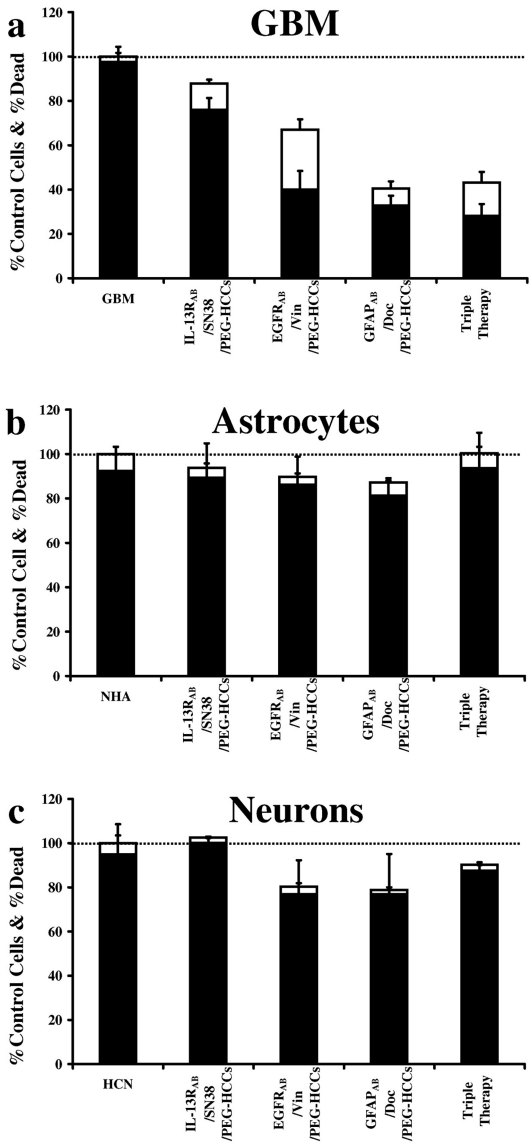

Figure 4. HADES triple therapy is not overly toxic toward astrocytes and neurons, but is highly toxic toward GBM. The living and dead cell numbers resulting from HADES treatment using 0.5 μM drug (Vin, Doc, and SN-38) targeted with monoclonal antibodies to GBM surface antigens (Il-13R, EGFR, and GFAP), (a) as IgG/drug/PEG–HCCs in cultures of GBM, (b) astrocytes, and (c) neurons. Black bars are % control living cells; white bars are % dead cells (GBM: $n = 8$ wells; NHA: $n = 8$ wells; HCN: $n = 4$ wells; error bars SD in all cases).

METHODS

HCCs Functionalization, Drug Loading, and Antibody Binding. The HCCs, PEG–HCCs, and drug/PEG–HCCs were prepared as reported by Berlin *et al.*[4] Drugs were dissolved in a minimal amount of methanol (for Vin and Doc) or THF (for SN-38) and added dropwise into a stirring aqueous solution of PEG–HCCs. After overnight sonication, the organic solvent was removed by rotary evaporating one-third of the original volume of solution,

adding one-third volume of water, and carrying out the same protocol evaporation/addition of water two more times according to published protocols.[3] Vin (LogP 4.8) was incorporated into PEG−HCCs with a mass ratio of 5:1, Doc (LogP 2.92) was incorporated into PEG−HCCs with a mass ratio of 1.7:1, and SN-38 (LogP 1.87) was incorporated into PEG−HCCs with a mass ratio of 0.33:1. Three mouse monoclonal antibodies, IgGs with affinities to cancer cell surface epitopes GFAP (2A5), Il-13R (YY-23Z), and EGFR (528), were obtained from Santa Cruz Biotechnology (Santa Cruz, CA, USA). Prior to use, drug-loaded PEG−HCCs were vortexed for 15 min and then were co-incubated with IgG for 15 min before being diluted and added to cell media. We used a mass ratio of PEG−HCCs:IgG of 4.1:1 throughout. Although heterogeneous, the average molecular mass of PEG−HCCs is ~920 000, which gives rise to a molar PEG−HCCs:IgG ratio of 1:1.5. Assuming the binding distribution to be Poissonian, ~80% of PEG−HCCs have one or more IgGs bound. Visualization of mouse IgG was performed by incubating Alexa Fluor 594 goat anti-mouse IgG (Molecular Probes), overnight. The levels of Alexa Fluor-IgG were calibrated using a 5 μm thick, gelatin tissue phantom, entrapping 150 μg mL^{-1}/1 μM goat-IgG.[20]

Cell Cultures. Primary human glioblastoma or astrocytoma cells were prepared from tumors within 10 min of their excision. The tumors were broken up using a pipet and then grown in DMEM, 20% FBS, GlutaMax-I, sodium pyruvate, and Pen/Strep, for 2 weeks. After this time, and in all presented data, the same media was used, except that sodium pyruvate was omitted. NHA were obtained from Lonza (Walkersville, MD, USA) and HCN from the American Type Culture Collection (ATCC Manassas, VA, USA) and grown subject to their recommendations. NHA were grown in Astrocyte Basal Medium supplemented with 3% FBS, glutamine, insulin, fhEGF, GA-1000, and ascorbic acid. HCN were prepared using ATCC-formulated Dulbecco's modified Eagle's medium (cat# 30-2002) and supplemented with 10% FBS. GBM and NHA were grown to confluency in the appropriate media on Costar 96-well growth plates (Corning, NYC, NY, USA), and HCN were grown on 16-well Lab-Tek slide chambers (Nalge Nunc, Rochester, NY, USA). Cells were grown for 24 h in the presence/absence of all effectors, in a total volume of 250 μL.

Assays. The ability of PEG−HCCs to take up hydrophobic solutes compromises a large number of high-throughput proliferation assays. We find that many common reporter chromophore/fluorophores partition into PEG−HCCs and then undergo altered absorbance/fluorescence properties.[3,4] PEG−HCCs also interfere with peptide-bond chelated copper reduction of Folin-Ciocalteu reagent (phosphomolybdate/phosphotungstate), making the Lowery protein assay unsuitable.

Protein Measurement. Cell proliferation studies with PEG−HCCs included four HCN controls: 100 μM CCCP (100% cell death), saline vehicle, PEG−HCCs, and IgG/PEG−HCCs using monoclonal antibodies toward GFAP, IL-13R, or EGFR; three HADES treatments where PEG−HCCs loaded with the drugs Vin, Doc, or SN-38 were added to HCN with or without antibodies; and a final triple pairing with or without antibodies. After 24 h the cells were washed with PBS and solubilized using 0.1% SDS, and then the protein present in the well was measured using the Thermo Scientific micro bicinchoninic acid (BCA) assay kit (Waltham, MA, USA), and the data are displayed in Figure S4.

Cell Viability Measurements. The measurements and quantification of DNA 3′OH and blunt-ended breaks by use of the *dd*TUNEL and blunt-ended ligation were performed as described in our recent publications.[24,34] The biotinylated *dd*UTP and biotinylated blunt-ended oligonucleotide probe were visualized using Texas Red-labeled avidin. Cells were incubated with 500 nM Mitotracker Red (cat# M22425), 1 μM Hoechst 33258 (cat# H1398), and 100 nM Dead Green (cat# I10291), with reagents obtained from Molecular Probes (Eugene, OR, USA). The activity of caspase-3 in fixed, 0.1% Triton permeabilized cells was measured using the Molecular Probes R110-EnzChek assay kit (cat# E13184), incubating cells for 1 h at 37 °C. Signals from Dead Green/R110 and from Mitotracker were calibrated against known concentrations of liquid FITC−gelatin and Texas Red−gelatin and then against FITC/Texas Red gelatin tissue phantoms 5 μm in thickness.[24,28]

Viability Cut-off. Cells were counted at 4× magnification using a Nikon Eclipse TE2000-E fluorescent microscope equipped with a CoolSnap ES digital camera system (Roper Scientific) containing a CCD-1300-Y/HS 1392 × 1040 imaging array cooled by a Peltier device. Images were recorded using Nikon NIS-Elements software as JEP2000 files. Cells were deemed to be nonviable if they had Dead Green/Hoechst signals >5 times the level found in control cells and >4.2 times the level of *dd*TUNEL-labeled DNA 3′OH ends in control cells.

Conflict of Interest: The authors declare no competing financial interest.

Acknowledgment. The work at the Methodist Hospital Research Institute was funded by The Henry J. N. Taub Fund for Neurological Research, The Pauline Sterne Wolff Memorial Foundation, Golfers Against Cancer, and the Methodist Hospital Foundation. S. Lopez provided valuable technical support throughout the study; D. Livingston and D. James provided proof reading and comments. The support at Rice University was provided by the Mission Connect Mild Traumatic Brain Injury Consortium funded by the Department of Defense (W81XWH-08-2-0143); the Alliance for NanoHealth through a subcontract from the University of Texas Health Science Center, Houston, with funding from the Department of Defense (W8XWH-07-2-0101); and the Nanoscale Science and Engineering Initiative of the National Science Foundation under Award EEC-0647452 through the NSF Center for Biological and Environmental Nanotechnology.

Supporting Information Available: Additional figures covering toxicity, antigenic mapping, and the pattern of cell death. This material is available free of charge *via* the Internet at http://pubs.acs.org.

REFERENCES AND NOTES

1. Preusser, M.; de Ribaupierre, S.; Wöhrer, A.; Erridge, S. C.; Hegi, M.; Weller, M.; Stupp, R. Current Concepts and Management of Glioblastoma. *Ann. Neurol.* **2011**, *70*, 9–21.
2. Chakraborty, M.; Jain, S.; Rani, V. Nanotechnology: Emerging Tool for Diagnostics and Therapeutics. *Appl. Biochem. Biotechnol.* **2011**, *165*, 1178–1187.
3. Berlin, J. M.; Leonard, A. D.; Pham, T. T.; Sano, D.; Marcano, D. C.; Yan, S.; Fiorentino, S.; Milas, Z. L.; Kosynkin, D. V.; Price, B. K.; *et al*. Effective Drug Delivery, *In Vitro* and *In Vivo*, by Carbon-Based Nanovectors Noncovalently Loaded with Unmodified Paclitaxel. *ACS Nano* **2010**, *4*, 4621–4636.
4. Berlin, J. M.; Pham, T. T.; Sano, D. S.; Mohamedali, K. A.; Marcano, D. C.; Myers, J. N.; Tour, J. M. Noncovalent Functionalization of Carbon Nanovectors with an Antibody Enables Targeted Drug Delivery. *ACS Nano* **2011**, *8*, 6643–6650.
5. Sano, D.; Berlin, J. M.; Pham, T. T.; Marcano, D. C.; Valdecanas, D. R.; Zhou, G.; Milas, L.; Myers, J. N. Tour, J. M. Non-Covalent Assembly of Targeted Carbon Nanovectors Enables Synergistic Drug and Radiation Cancer Therapy *In Vivo*. *ACS Nano*, Just Accepted Manuscript, DOI: 10.1021/nn204885f.
6. Liu, Z.; Fan, A. C.; Rakhra, K.; Sherlock, S.; Goodwin, A.; Chen, X.; Yang, Q.; Felsher, D. W.; Dai, H. Supramolecular Stacking of Doxorubicin on Carbon Nanotubes for *In Vivo* Cancer Therapy. *Angew. Chem., Int. Ed.* **2009**, *48*, 7668–7672.
7. Hong, G.; Tabakman, S. M.; Welsher, K.; Chen, Z.; Robinson, J. T.; Wang, H.; Zhang, B.; Dai, H. Near-Infrared-Fluorescence-Enhanced Molecular Imaging of Live Cells on Gold Substrates. *Angew. Chem.* **2011**, *123*, 4740–4744.
8. O'Driscoll, C. M.; Griffin, B. T. Biopharmaceutical Challenges Associated with Drugs with Low Aqueous Solubility: The Potential Impact of Lipid-Based Formulations. *Adv. Drug Delivery Rev.* **2008**, *60*, 617–624.
9. Ohba, S.; Hirose, Y.; Yoshida, K.; Yazaki, T.; Kawase, T. Inhibition of 90-KD Heat Shock Protein Potentiates the Cytotoxicity of Chemotherapeutic Agents in Human Glioma Cells. *J. Neurosurg.* **2010**, *112*, 33–42.
10. Biggs, T.; Foreman, J.; Sundstrom, L.; Regenass, U.; Lehembre, F. Antitumor Compound Testing in Glioblastoma Organotypic Brain Cultures. *J. Biomol. Screening* **2011**, *16*, 805–817.

11. Wang, W.; Ghandi, A.; Liebes, L.; Louie, S. G.; Hofman, F. M.; Schönthal, A. H.; Chen, T. C. Effective Conversion of Irinotecan to SN-38 after Intratumoral Drug Delivery to an Intracranial Murine Glioma Model *in vivo*. Laboratory Investigation. *J. Neurosurg.* **2011**, *114*, 689–694.
12. Maurya, D.; Ayuzawa, R.; Doi, C.; Troyer, D.; Tamura, M. Topoisomerase I Inhibitor SN-38 Effectively Attenuates Growth of Human Non-Small Cell Lung Cancer Cell Lines *In Vitro* and *In Vivo*. *J. Environ. Pathol. Toxicol. Oncol.* **2011**, *30*, 1–10.
13. Hoshino, T.; Wilson, C. B.; Muraoka, I. The Stathmokinetic (Mitostatic) Effect of Vincristine and Vinblastine on Human Gliomas. *Acta Neuropathol.* **1979**, *47*, 21–25.
14. Fabbri, F.; Amadori, D.; Carloni, S.; Brigliadori, G.; Tesei, A.; Ulivi, P.; Rosetti, M.; Vannini, I.; Arienti, C.; Zoli, W.; *et al*. Mitotic Catastrophe and Apoptosis Induced by Docetaxel in Hormone-Refractory Prostate Cancer Cells. *J. Cell. Physiol.* **2008**, *217*, 494–501.
15. Zhang, J. A.; Xuan, T.; Parmar, M.; Ma, L.; Ugwu, S.; Ali, S.; Ahmad, I. Development and Characterization of a Novel Liposome-Based Formulation of SN-38. *Int. J. Pharm.* **2004**, *270*, 93–107.
16. Chekhonin, V.; Baklaushev, V.; Yusubalieva, G.; Gurina, O. Targeted Transport of ^{125}I-Labeled Antibody to GFAP and AMVB1 in an Experimental Rat Model of C6 Glioma. *J. Neuroimmune Pharm.* **2009**, *4*, 28–34.
17. Husain, S. R.; Joshi, B. H.; Puri, R. K. Interleukin-13 Receptor as a Unique Target for Anti-Glioblastoma Therapy. *Int. J. Cancer* **2011**, *92*, 168–175.
18. Eng, L. F.; Ghirnikar, R. S. GFAP and Astrogliosis. *Brain Pathol.* **1994**, *4*, 229–237.
19. Schittenhelm, J.; Mittelbronn, M.; Nguyen, T.-D.; Meyermann, R.; Beschorner, R. WT1 Expression Distinguishes Astrocytic Tumor Cells from Normal and Reactive Astrocytes. *Brain Pathol.* **2008**, *18*, 344–353.
20. Wu, H.; Mahmood, A.; Lu, D.; Jiang, H.; Xiong, Y.; Zhou, D.; Chopp, M. Attenuation of Astrogliosis and Modulation of Endothelial Growth Factor Receptor in Lipid Rafts by Simvastatin After Traumatic Brain Injury. *J. Neurosurg.* **2010**, *113*, 591–597.
21. Hatanpaa, K. J.; Burma, S.; Zhao, D.; Habib, A. A. Epidermal Growth Factor Receptor in Glioma: Signal Transduction, Neuropathology, Imaging, and Radioresistance. *Neoplasia* **2010**, *12*, 675–684.
22. Chekhonin, V. P.; Baklaushev, V. P.; Yusubalieva, G. M.; Belorusova, A. E.; Gulyaev, M. V.; Tsitrin, E. B.; Grinenko, N. F.; Gurina, O. I.; Pirogov, Y. A. Targeted Delivery of Liposomal Nanocontainers to the Peritumoral Zone of Glioma by Means of Monoclonal Antibodies Against GFAP and the Extracellular Loop of Cx43. *Nanomed: Nanotech. Biol. Med*. **2011**, Epub ahead of print,http://www.ncbi.nlm.nih.gov/pubmed/21703991.
23. Worle-Knirsch, J. M.; Pulskamp, K.; Krug, H. F. Oops They Did It Again! Carbon Nanotubes Hoax Scientists in Viability Assays. *Nano Lett.* **2006**, *6*, 1261–1268.
24. Baskin, D. S.; Widmayer, M. A.; Sharpe, M. A. Quantification of DNase Type I Ends, DNase Type II Ends, and Modified Bases Using Fluorescently Labeled ddUTP, Terminal Deoxynucleotidyl Transferase, and Formamidopyrimidine-DNA Glycosylase. *Biotechniques* **2010**, *49*, 505–512.
25. Frank, S.; Steffens, S.; Fischer, U.; Tlolko, A.; Rainov, N. G.; Kramm, C. M. Differential Cytotoxicity and Bystander Effect of the Rabbit Cytochrome P450 4B1 Enzyme Gene by Two Different Prodrugs: Implications for Pharmacogene Therapy. *Cancer Gene Ther.* **2002**, *9*, 178–88.
26. Morelock, M. M.; Hunter, E. A.; Moran, T. J.; Heynen, S.; Laris, C.; Thieleking, M.; Akong, M.; Mikic, I.; Callaway, S.; DeLeon, R. P.; *et al*. Statistics of Assay Validation in High Throughput Cell Imaging of Nuclear Factor Kappaβ Nuclear Translocation. *Assay Drug Dev. Technol.* **2005**, *3*, 483–499.
27. Nakatsu, S.; Kondo, S.; Kondo, Y.; Yin, D.; Peterson, J. W.; Kaakaji, R.; Morimura, T.; Kikuchi, H.; Takeuchi, J.; Barnett, G. H. Induction of Apoptosis in Multi-Drug Resistant (MDR) Human Glioblastoma Cells by SN-38, a Metabolite of the Camptothecin Derivative CPT-11. *Cancer Chemother. Pharmacol.* **1997**, *39*, 417–423.
28. Baskin, D. S.; Widmayer, M. A.; Sharpe, M. A. Quantification and Calibration of Images in Fluorescence Microscopy. *Anal. Biochem.* **2010**, *404*, 118–126.
29. Upreti, M.; Lyle, C. S.; Skaug, B.; Du, L.; Chambers, T. C. Vinblastine-Induced Apoptosis is Mediated by Discrete Alterations in Subcellular Location, Oligomeric Structure, and Activation Status of Specific Bcl-2 Family Members. *J. Biol. Chem.* **2006**, *281*, 15941–15950.
30. Huang, Y. T.; Huang, D. M.; Guh, J. H.; Chen, I. L.; Tzeng, C. C.; Teng, C. M. CIL-102 Interacts with Microtubule Polymerization and Causes Mitotic Arrest Following Apoptosis in the Human Prostate Cancer PC-3 Cell Line. *J. Biol. Chem.* **2005**, *280*, 2771–2779.
31. Wang, G. J.; Jackson, J. G.; Thayer, S. A. Altered Distribution of Mitochondria Impairs Calcium Homeostasis in Rat Hippocampal Neurons in Culture. *J. Neurochem.* **2003**, *87*, 85–94.
32. Hickson, J.; Ackler, S.; Klaubert, D.; Bouska, J.; Ellis, P.; Foster, K.; Oleksijew, A.; Rodriguez, L.; Schlessinger, S.; Wang, B.; *et al*. Noninvasive Molecular Imaging of Apoptosis *In Vivo* Using a Modified Firefly Luciferase Substrate, Z-DEVD-Aminoluciferin. *Cell. Death Differ.* **2010**, *17*, 1003–1010.
33. Boland, B.; Kumar, A.; Lee, S.; Platt, F. M.; Wegiel, J.; Yu, W. H.; Nixon, R. A. Autophagy Induction and Autophagosome Clearance in Neurons: Relationship to Autophagic Pathology in Alzheimer's Disease. *J. Neurosci.* **2008**, *28*, 6926–6937.
34. Wagner, B.; Natarajan, A.; Grünaug, S.; Kroismayr, R.; Wagner, E. F.; Sibilia, M. Neuronal Survival Depends on EGFR Signaling in Cortical But Not Midbrain Astrocytes. *Eur. Mol. Biol. Org. J.* **2006**, *25*, 752–762.
35. Fillmore, H. L.; Shultz, M. D.; Henderson, S. C.; Cooper, P.; Broaddus, W. C.; Chen, Z. J.; Shu, C. Y.; Zhang, J. F.; Ge, J. C.; Dorn, H. C.; *et al*. Conjugation of Functionalized Gadolinium Metallofullerenes with IL-13 Peptides for Targeting and Imaging Glial Tumors. *Nanomedicine* **2011**, *6*, 449–458.
36. Tateki Kubo, T.; Yamashita, T.; Yamaguchi, A.; Sumimoto, H.; Hosokawa, K; Tohyama, M. A Novel FERM Domain Including Guanine Nucleotide Exchange Factor Is Involved in Rac Signaling and Regulates Neurite Remodeling. *J. Neurosci.* **2002**, *22*, 8504–8513.